HEAT AND MOMENTUM TRANSFER IN THE WALL REGION OF A CYLINDRICAL VESSEL MIXED BY A TURBINE IMPELLER*

Ivan FOŘT[a], Jiří PLACEK[b], Frederyk STREK[c], Zdislaw JAWORSKI[c] and Joana KARCZ[c]

[a] *Department of Chemical Engineering,*
Prague Institute of Chemical Technology, 166 28 Prague 6
[b] *Microbiological Institute,*
Czechoslovak Academy of Sciences, 140 00 Prague 4 and
[c] *Department of Chemical Engineering,*
Polytechnic Institute, Szczecin, 71—065 Szczecin, Poland

Received July 6th, 1977

Velocity and temperature fields have been described in the wall region of a cylindrical vessel equipped with radial baffles mixed by a standard six-blade disc turbine impeller under the turbulent regime of the flow in a homogeneous Newtonian charge. The results of experiments offer conclusions regarding the mechanism of the turbulent flow in individual subregions of the wall region together with the method of description of the flow in these regions as a sequence of impinging wall turbulent streams. Based on the theory of analogy the results on the turbulent heat and momentum transfer have been compared and confirm validity of the Chilton–Colburn analogy in which the characteristic quantities for the calculation of the local friction factor are parameters of the wall region flow — the characteristic velocity and the characteristic thickness of the wall region.

Mechanical mixing of liquids is usually carried out with the aim to intesify heat and/or mass transfer in technological apparatuses. If need arises to exchange heat with the surroundings the heat transfer in the bulk liquid is complicated by heat transfer through the surface between the charge and the heat transfer medium (*e.g.* coolant) separated from the charge by the exchange surface. Since the intensity of heat transfer on the side of the charge may be affected by its flow it is necessary to know the mechanism of convective transfer in this region. The knowledge of the velocity field near the vessel's wall leads in turn to the description of heat transfer between the wall and the mixed charge.

The problem of analogy between momentum transfer on the one hand and heat or mass transfer between the wall of a mixing vessel and the mixed liquid on the other hand has been closely examined by several authors: Askew and Beckman[1] found that the effect of angular coordinate φ (see below) between two neighbouring baffles on the local value of the wall-to-liquid heat transfer coefficient is insignificant while the effect of the axial coordinate, z_M, is considerable.

* Part L in the series Studies on Mixing; Part IL: This Journal *43*, 3148 (1978). Presented at the VIth International CHISA Congress, Prague 1978.

By their not quite perfect experimental technique they evaluated the field of velocities and local heat transfer coefficients to point at mutual correlation of these two quantities. Akse and coworkers[2] carried out detailed experiments to determine the temperature field in the wall of the vessel and found that maximum values of the heat transfer coefficient are reached in the proximity of the horizontal plane of symmetry of the turbine impeller (*i.e.* in the plane of the disc of the turbine), where the axial coordinate assumes values from the interval $(-h/2, h/2)$. In this region, the so called region of impinging jet, the authors evaluated the exponent over the Reynolds number for mixing in the power-law expression for heat transfer by forced convection. This exponent amounted to one half while in the remaining parts of the wall (in the region of the wall jet) it equalled to three quarters. Le Lan and coworkers[3-5] paid special attention to the effect of axial coordinate, z_M, on the local wall-to-liquid mass transfer coefficient to find that it decreases from the horizontal plane of $z_M = 0$ with almost first power of this coordinate. More detailed studies of the shear stress distribution (using Preston's tube) as well as heat transfer coefficient distribution have been carried out by Stammers[6]. His results, though carying an error caused by the presence of a large probe in the wall region, revealed an important fact for the determination of local heat transfer coefficient by an instrument measuring localized values of intensity of heat transfer: in comparisons of the mean and the local heat transfer coefficients the local value must be corrected on the different thickness of the thermal boundary layer. This thickness in case of the mean transfer coefficient corresponds to the whole transfer surface, beginning at the point $z_M = 0$, while in case of the localized value it corresponds to the heated surface at the point given by the position of the instrument, *i.e.* at points with different coordinate z_M. As far as the analogy between the wall-to-liquid momentum and heat transfer is concerned as most comprehensive appear the data of Mizushina and coworkers[7]. These authors proved validity of the Chilton–Colburn analogy between heat and momentum transfer for a system without baffles and proved a significant role played by the peripheral velocity of the blades in affecting intensity of heat transfer in the charge. For systems with baffles it was the papers of Askew and Beckman[1] and Le Lan and Angelino[5] from which one can also infer on the validity of the above mentioned analogy although the extent of experiments and the experimental technique did not allow to present their findings with sufficient veritability.

THEORETICAL

Consider a mixed system (Fig. 1) consisting of a cylindrical vessel with a flat bottom, equipped with four radial baffles reaching to the bottom, their width, b, being one tenth of the inner diameter, D. The vessel is filled with a Newtonian charge up to a height H and mixed by a standard six-blade disc turbine impeller with vertical blades located coaxially with the vessel. The diameter of the impeller is d and its is located at a height H_2, or H'_2 above the bottom. Let us choose a cylindrical frame of reference (see Fig. 2) with the coordinate designated r, φ, z, attached to the system. In this system the radial coordinate is zero on the wall of the mixed vessel and the coordinate z equals unity at the bottom. There is another coordinate, z_M, introduced with a zero value at the point where the axis of the vessel intersects with the horizontal plane of the disc of the impeller. The plane of zero angular coordinate is one containing any two baffles located on the opposite side of the circumference; it takes positive values in the direction of rotation of the impeller.

The character of the flow of the charge is turbulent. Local values of the mean velocity $\bar{\mathbf{w}}$ at the point 0 (Fig. 2) are shown by an oriented segment of a line whose rectangular projection onto a vertical axial plane is the component $\bar{\mathbf{w}}_k$. The direction is then given by two angles in the basis $\mathbf{e}_r$, $\mathbf{e}_\varphi$, $\mathbf{e}_z$ – the angle alpha made by the unit vector $\mathbf{e}_z$ and the rectangular projection of the velocity $\bar{\mathbf{w}}_k$, and, by angle beta made by the mean velocity and its projection $\bar{\mathbf{w}}_r$. The velocity $\bar{\mathbf{w}}$ then has the following components in the basis $\mathbf{e}_r$, $\mathbf{e}_\varphi$, $\mathbf{e}_z$: a radial component $\bar{w}_r$, its direction being identical with the direction of the element of the basis $\mathbf{e}_r$, a tangential component, $\bar{w}_\varphi$, its direction being identical with the element of the basis $\mathbf{e}_\varphi$ and an axial component $\bar{w}_z$, identical as to the direction with that of the element of the basis $\mathbf{e}_z$.

Heat transfer between the wall and the mixed liquid is controlled, according to the general description of the convective transfer in the wall region[8,9], by momentum transfer in the boundary layer immediately adjacent to the wall. The field of velocities near the wall (Fig. 3) may be characterized by two hydrodynamic parameters[10,11] of the radial profile of the axial mean velocity component $\bar{w}_z = \bar{w}_z(r)$: the maximum value $\bar{w}_{z,\max}$ (the so-called velocity scale) and the radial coordinate of this maximum σ (the so-called length scale). Both scales vary along the wall, *i.e.* with the axial and the

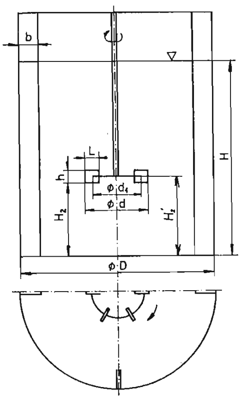

FIG. 1

Mixed System with Standard Disc Turbine Impeller

$(H/D = 1;\ H_2'/D = 1/3,\ \ d : d_1 : L : h = 20 : 15 : 5 : 14,\ d/D = 1/4;\ 1/3)$.

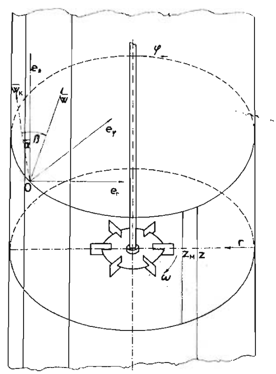

FIG. 2

Frame of Reference in the Mixed System

tangential coordinate, and depend also on the size of the impeller and the frequency of its revolution. In terms of these two quantities, characterizing the wall region flow, one can calculate local values of the friction factor on the wall, for which the following correlation has been obtained from experiments models of such flows[12]

$$c_f = 0{\cdot}0565 \,\mathrm{Re}^{-0{,}25} . \tag{1}$$

The local value of the Reynolds criterion has been defined by means of the above introduced scales and the kinematic viscosity of the charge as

$$\mathrm{Re} \equiv \bar{w}_{z,\max}\, \sigma/\nu . \tag{2}$$

The knowledge of the velocity field in the wall region flow may be used to assess the temperature distribution in this region. In view of the fact that the flow of the charge in the wall region may be regarded as turbulent, it is permisible to admit the Chilton–Colburn analogy[13] between the heat and momentum transfer in the form

$$c_f = j_h = \mathrm{St}\,\mathrm{Pr}^{2/3} . \tag{3}$$

Local values of the Nusselt, Reynolds and Prandtl number are related by

$$\mathrm{Nu} = 0{\cdot}0565 \,\mathrm{Re}^{3/4}\,\mathrm{Pr}^{1/3} . \tag{4}$$

Substituting appropriate hydrodynamic and thermal quantities into the expressions for the Reynolds and the Nusselt groups one obtains finally an unambiguous relation between local values of the velocity and the thermal field in the form

$$\alpha_a = 0{\cdot}0565(\lambda/\sigma^{1/4})\,(\bar{w}_{z,\max}/\nu)^{3/4}\,\mathrm{Pr}^{1/3} . \tag{5}$$

The quantity λ in Eq. (5) is the thermal conductivity of the mixed charge and α_a is the local heat transfer coefficient obtained from analogy between heat and momentum transfer in the examined region.

EXPERIMENTAL

The aim of the performed experiments was to prove Eq. (5), characterizing quantitatively the examined analogy. For this purpose two series of experiments were carried out on virtually identical set-ups, under identical hydrodynamic conditions characterized by identical values of the Reynolds number for mixing, $\mathrm{Re_M}$, and identical values of the simplexes of geometrical similarity (H/D, d/D, H_2/D, b/D, type of impeller). These experiments were designed to determine radial profiles of the axial component of mean velocity and local heat transfer coefficients α_m between the wall and the charge.

The hydrodynamic study involved experiments with threads[14], indicating time-averaged value of the angle alpha (always from about 70 instantaneous positions) as well as experiments with a miniaturized Pitot tube[15] (Figs 4 and 5). The latter experiments served to determine for the already known value of alpha the radial profiles of the quantity β and $|\bar{\mathbf{w}}|$ in the wall region. The inspected points in the wall region (*e.g.* point 0 in Fig. 2) were located on three vertical planes passing through the axis given by the angular coordinate $\varphi = 22{\cdot}5$, 45 and $67{\cdot}5°$. There were a total of six such points along the height: One in the horizontal plane of symmetry of the impeller, the other 30 mm below and in four positions above this plane with the vertical spacing being always 36 mm. The velocity fields were thus examined in a total

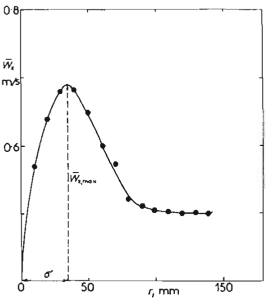

FIG. 3

Radial Profile of Axial Mean Velocity Component Near the Wall

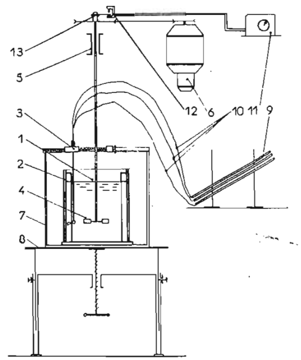

FIG. 4

Scheme of the Set-Up to Measure Local Velocities

1 Vessel ($D = 290$ mm), 2 clamp, 3 support, 4 impeller, 5 bearings, 6 electromotor and tachodynamo, 7 thermostat, 8 bench with rectractable board, 9 manometers, 10 tubings among the Pitot tube and manometers, 11 revolution counter of Tesla BM 445 E 11 type, 12 photoelectric detector of impeller revolution of Tesla BP 3620 type, 13 light beam shopper.

of 18 positions between two adjacent baffles, namely in three positions below the horizontal plane of symmetry of the impeller, in three positions on the plane of symmetry alone and in 12 positions between this plane of symmetry and the liquid level. The radial profiles obtained served to evaluate graphically the quantities $\bar{w}_{z,max}$ and σ (Fig. 3); the axial component of local mean velocity, $\bar{w}_z$, was computed from the measured values $|\bar{\mathbf{w}}|$, α and β by means of the following transformation formula

$$\bar{w}_z = |\bar{\mathbf{w}}| \cos \alpha \cos \beta \,. \tag{6}$$

The relative accuracy of determination of the velocity scale $\bar{w}_{z,max}$ was estimated to be 15% of the measureed value and the absolute error of the length scale σ was 0·5 mm.

The determination of the local coefficients of heat transfer was carried out on an equipment with retractable bottom (Fig. 6) with the aid of an instrument detecting thermal flux (Fig. 7). The equipment contained three thermocouples copper-constantan to detect the thermal flux q (thermocouples b and d) and to detect the temperature difference between the wall and the mixed liquid (thermocouple c). The temperature of the liquid was taken to be the arithmetic average of the reading of a total of seven thermocouples immersed in the liquid. The local value of the heat transfer coefficient α_m was evaluated from the detected quantities by means of the Newton law

$$\alpha_m = p \frac{q}{\Delta t} = p \frac{\lambda}{l_2} \frac{\Delta t_2}{\Delta t - (l_1/(l_2)) \Delta t_2} \,. \tag{7}$$

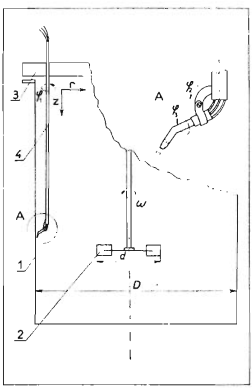

FIG. 5

Adjustment of Three-Opening Pitot Tube

1 Wall, 2 turbine, 3 support, 4 clamp; φ_1 angle of rotation of the clamp in the support, φ_2, φ_3 angles of the inclination and rotation of probe in the clamp.

The difference, Δt_1, in Eq. (7) characterized the temperature difference between the thermocouple c at the distance l_1 in the radial direction frcm the wall and the mixed liquid; the difference Δt_2 characterizes the temperature difference between the thermocouples b and d which are radially l_2 apart. The quantity λ is the thermal conductivity of a stainless steel from which the wall was manufactured. Its value was determined by calibration in the given geometrical configuration with a quiescent liquid (the motionless impeller) when the process of heating the charge was regarded to be governed by free convection[16].

The parameter p characterizing the different position of the beginning of the thermal and hydrodynamic boundary layer was estimated on the basis of the above presented concept of the flow in the wall region and the relation (*1*) for the local friction factor (see Appendix). The design of the apparatus ensured two-dimensional flow of heat from the source perpendicularly to the wall, *i.e.* in the radial direction, while the heat flux in the direction along the wall was eliminated by auxiliary sources of heat surounding the instrument itself (Fig. 7). This configuration permitted the local heat transfer coefficient to be determined to the accuracy of $\pm 15\%$.

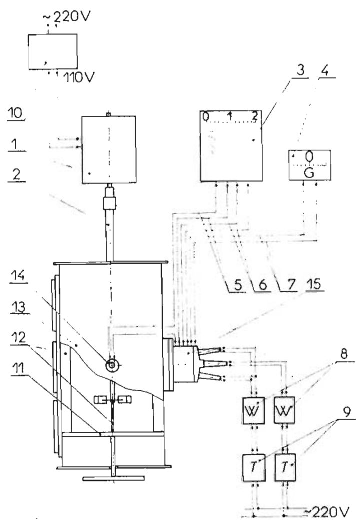

FIG. 6

Scheme of the Set-Up to Measure Local Heat Transfer Coefficient

1 Electromotor and tachodynamo, **2** shaft and impeller, **3** point chart recorder (measurement of voltage), **4** galvanometer (thermal flux), **5** measurement of voltage between point c and liquid, **6** measurement of voltage between points b and d, **7** measurement of voltage between the surroundings and the heat flux instrument, **8** wattmeters, **9** transformers, **10** frequency regulator, **11** rectractable bottom, **12** radial baffle, **13** vessel ($D = 282$ mm), **14** thermocouple leads, **15** heat flux measuring instrument.

RESULTS AND DISCUSSION

Typical experimental values of $\bar{w}_{z,max}$ and σ are shown in Table I. The distribution of the angles α along the wall found by the tracer threads showed a marked influence of the tangential component of velocity on the magnitude of the resulting velocity in the examined region. The deviation from the axial direction amounted on average to 20° in the direction of rotation of impeller blades; it was only in the proximity of the level past the baffle where the direction of the resulting velocity was reversed due to the action of the vortex. Values of the velocity and the length scales then vary along the wall systematically reaching extreme values (the length scale a minimum, the velocity scale a maximum) in the neighbourhood of the axial coordinate $z_M = 0$. The change of both scales with the coordinate z_M may be expressed by the relations[10,11]

$$\bar{w}_{z,max} = C_1 z_M^a , \quad \sigma = C_2 z_M^b . \tag{8a, b}$$

Exponents a, b were evaluated from experimental data in the following intervals: a ⟨0·55; 0·6⟩, b ⟨1·60; 2·20⟩. This points out the fact that the velocity profile $\bar{w}_z = \bar{w}_z(r)$ develops not only in the region of impinging jet (where in our set-up $z_M < 20$ mm) but in the whole wall region (in our set-up $z_M > 20$ mm). This fact makes the flow of the mixed liquid along the walls somewhat different from current cases of wall jet flows described in the literature[10-12].

TABLE I

Velocity and Length Scales in the Wall Region $(d/D) = 1/4$; $Re_M = 7.5 \cdot 10^4$)

z_M, nm	$\bar{w}_{z,max}$, m s^{-1}/σ, mm		
	$\varphi = 67.5°$	$\varphi = 45°$	$\varphi = 22.5°$
−74	0·604/9·0	0·658/7·0	0·756/3·5
−55·5	0·660/4·0	0·737/4·0	0·750/3·0
−37	0·403/2·5	0·779/2·5	0·839/2·5
−18·5	0·566/2·5	0·650/2·0	0·683/2·0
18·5	0·700/2·5	0·675/2·5	0·661/2·0
37	0·859/2·5	1·012/2·0	0·854/2·5
55·5	0·655/2·5	0·638/2·5	0·665/2·5
74	0·719/4·5	0·751/3·5	0·692/2·5
111	0·519/7·5	0·555/5·0	0·471/4·8
148	0·352/9·0	0·378/13·0	0·311/16·0

The results of thermal measurements was a sequence of local values of heat transfer coefficients α_m between the wall and the flowing charge (see examples in Figs 8) always for a given d/D and Re_M (given by the frequency of revolution of the impeller, the impeller diameter d and the kinematic viscosity of the charge ν). From these results it follows that although the introduced characteristics $\bar{w}_{z,max}$ and σ markedly depend on the angular coordinate φ (Table I), the heat transfer coefficient practically does not, *i.e.* remains unaffected by the baffles within the experimental error. This coefficient, however, strongly depends on the axial acoordinate z (or z_M): in region of the impinging jet where the streamlines change their direction from predominantly radial (away from the impeller) into predominantly axial one (toward the level or the bottom), where a boundary layer forms on the wall, the local heat transfer coefficients are twice those in region of the wall jet, *e.g.* in the proximity of the level. This suggests that from the standpoint of maximum intensity of wall-to--liquid heat transfer the optimum position of the impeller is half way between the bottom and the level. In this configuration the mean value of the heat transfer coefficient over the whole surface is maximum. Let us note still that α_m obtained as an integral mean over the whole surface of the wall agrees to within 10% in all four cases with the heat transfer coefficient computed from the correlations published for the given arrangement in the literature[17].

As a next step the two series of corresponding local heat transfer coefficients: directly measured and computed for analogy between heat and momentum transfer, were compared (see examples in Fig. 9 and 10) statistically. The statistical test[18] involved sets of 18 values of the local coefficients α_i ($i = m, a$) for all investigated experimental conditions (*i.e.* for two levels of relative size of the impeller $d/D = 1/4$

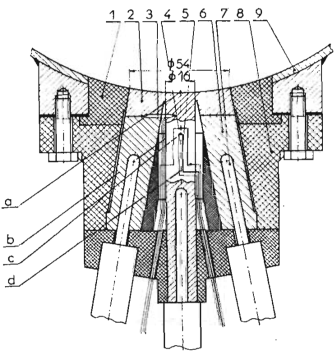

FIG. 7

Scheme of Instrument to Measure Heat Flux
1 Teflon part of jacket, **2** internal part, **3** thermocouples to detect thermal flux, **4** thermocouple ***b***, **5** thermocouple ***c***, **6** part to eliminate thermal flux along vessel's walls, **7** auxiliary heat sources uniformly spaced around the central part of instrument (total number 8), **8** textolite part of jacket, **9** wall of vessel, a inner surface of vessel wall

and 1/3 and always two levels of the frequency of revolution) and proved the hypothesis of the identity of the two sets. Accordingly, the model of the mechanism of convective heat transfer between the wall and the liquid mixed by a standard turbine impeller has been proved experimentally. The regime of the flow is fully turbulent as in all experiments performed the Reynolds number for mixing exceeded $5 \cdot 0 . 10^4$.

APPENDIX

The parameter p from Eq. (7), characterizing different position of the beginning of the thermal and hydrodynamic boundary layer near the wall was evaluated for the given set-up using the following arguments: Consider the flow of a mixed liquid along the wall of a cylindrical vessel between two adjacent baffles. In the origin of the used frame of reference ($z_M = r = 0$) appears the hydrodynamic and, in case of heating the whole wall to a constant temperature, also the thermal boundary layer. The flow is regarded to be two-dimensional (coordinates r, z_M and velocity components $\bar{w}_z$ and $\bar{w}_r$) and radial heat transfer to be significantly more intensive than the axial one. The heat transfer in the thermal boundary layer may be then expressed from the

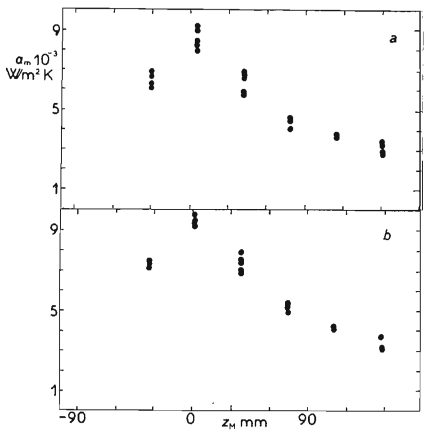

FIG. 8

Local Heat Transfer Coefficient as a Function of Axial and Angular Coordinate
a $d/D = 1/4$, $Re_M = 5 \cdot 26 . 10^4$, *b* $d/D = 1/3$, $Re_M = 6 \cdot 36 . 10^4$.

Fourier–Kirchhoff equation[13] in the form

$$\overline{w}_r \frac{\partial t}{\partial r} + \overline{w}_z \frac{\partial t}{\partial z_M} = a \frac{\partial^2 t}{\partial r^2} . \tag{9}$$

In the considered region also the equation of continuity applies which for an incompressible fluid and two-dimensional flows takes the form

$$\frac{\partial \overline{w}_r}{\partial r} + \frac{\partial \overline{w}_z}{\partial z_M} = 0 . \tag{10}$$

In Eqs (*9*) and (*10*) we shall neglect the curvature of the wall and for Eq. (*9*) we shall assume, in addition, that the thickness of the thermal boundary layer is substantially smaller than that of the hydrodynamic layer. Hence for the thermal conductivity may take only its molecular value neglecting thus the turbulent transport. This assumption is not unjustified as the thicknesses of the thermal boundary layer Δ_z and the hydrodynamic boundary layer, δ_z, are related by[13]

$$\Delta_z = \delta_z/\mathrm{Pr}^{1/3} ; \tag{11}$$

the value of the Prandtl number for liquids is substantially greater than unity.

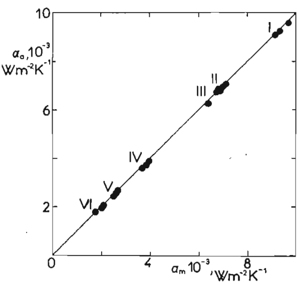

FIG. 9

Comparison of Experimental Heat Transfer Coefficients α_m with α_a predicted by Chilton–Colburn Analogy ($d/D = 1/4$; $\mathrm{Re}_M = 5{\cdot}26 . 10^4$)

Points I $Z_M = 5$ mm, II —31 mm, III 41 mm, IV 77 mm, V 113 mm, VI 149 mm.

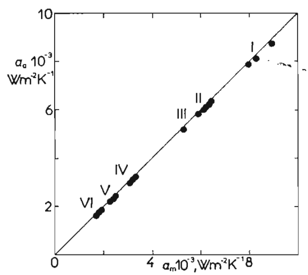

FIG. 10

Comparison of Experimental Heat Transfer Coefficients α_m with α_a predicted by Chilton–Colburn Analogy ($d/D = 1/3$; $\mathrm{Re}_M = 6{\cdot}36 . 10^4$)

Points I $Z_m = 22{\cdot}5$ mm, II —33·5 mm, III 38·5 mm, IV 74·5 mm, IV 110·5 mm, VI 146·5 mm.

The components of the mean velocity in Eqs (*9*) and (*10*) shall be expressed with the aid of the quantity

$$F_z = (\partial \bar{w}_z/\partial r)_{r=0}\,, \tag{12}$$

which may be regarded to be approximately constant for our thermal boundary layer. Thus we have

$$\bar{w}_z = F_z \, . \, r \tag{13a}$$

and with the aid of Eq. (*10*) for the other velocity component

$$\bar{w}_r = -(F'_z/2)\, r^2\,. \tag{13b}$$

Let us introduce following dimensionless parameters — the thickness of the thermal boundary layer r/Δ_z and the dimensionless temperature $T = (t - t_\infty)/(t_0 - t_\infty)$ where t_0 designates the temperature of the wall and t_∞ the integral-mean temperature of the mixed charge. On assuming the dependence between the just defined variables in the form of the infinite power series as

$$T = \sum_{N=0}^{\infty} a_N \left(\frac{r}{\Delta_z}\right)^N, \tag{14}$$

Eq. (*9*) may be expressed, after transformations, in the form

$$\frac{\bar{w}_r}{\Delta_z} \sum_{N=1}^{\infty} N a_N \left(\frac{r}{\Delta_z}\right)^{N-1} - \frac{\bar{w}_z \Delta'_z}{\Delta_z} \sum_{N=1}^{\infty} N a_N \left(\frac{r}{\Delta_z}\right)^N = \frac{a}{\Delta_z^2} \sum_{N=2}^{\infty} N(N-1)\, a_N \left(\frac{r}{\Delta_z}\right)^{N-2}, \tag{15}$$

or, after introducing the quantity F_z, in the form

$$-\frac{F'_z \Delta_z}{2} \sum_{N=1}^{\infty} N a_N \left(\frac{r}{\Delta_z}\right)^{N+1} - F_z \Delta'_z \sum_{N=1}^{\infty} N a_N \left(\frac{r}{\Delta_z}\right)^{N+1} = \frac{a}{\Delta_z^2} \sum_{N=2}^{\infty} N(N-1)\, a_N \left(\frac{r}{\Delta_z}\right)^{N-2}. \tag{16}$$

Integration of Eq. (*16*) with respect to the variable r/Δ_z in the limits 0 and 1, *i.e.* across the thickness of the thermal boundary layer we obtain

$$-\left(\frac{F'_z \Delta_z}{2} + F_z \Delta'_z\right) \sum_{n=1}^{\infty} \frac{N a_N}{N+2} = \frac{a}{\Delta_z^2} \sum_{N=2}^{\infty} N a_N\,, \tag{17}$$

or, after some rearrangement

$$\frac{3}{2} F_z' \Delta_z^3 + F_z(\Delta_z^3)' = -3a \sum_{N=2}^{\infty} N a_N / [\sum_{N=1}^{\infty} N a_N/(N+2)] = A\,. \tag{18}$$

The quantity A on the right hand side of Eq. (*18*) is not a function of the coordinate z so that after double integrating we obtain finally

$$\Delta_z^3 = A F_z^{-3/2} \int_{z_{MO}}^{z_M} F_z^{1/2} dz_M\,, \tag{19}$$

where the coordinate z_{MO} characterizes the beginning of the thermal boundary layer in the wall region. In view of the definition of the shear stress on the wall

$$\bar{\tau}_0 = c_f \,.\, 1/2(\bar{w}_{z,\max}^2)\, \varrho \tag{20}$$

and Eq. (*1*) for the friction factor c_f we obtain

$$\bar{\tau}_0 = 0{\cdot}0565 \; \mathrm{Re}^{-0.25} \,.\, 1/2(\bar{w}_{z,\max}^2)\, \varrho\,. \tag{21}$$

Since

$$\bar{\tau}_0 \approx \varrho \nu \left(\frac{\partial \bar{w}_z}{\partial r}\right)_{r=0} = \varrho \nu F_z\,, \tag{22}$$

we have for the quantity F_z the relation

$$F_z = 0{\cdot}0565 \; \mathrm{Re}^{-0.25} \, \bar{w}_{z,\max}^2 / 2\nu\,. \tag{23}$$

The wall-to-liquid heat transfer coefficient relates to the temperature field in the charge in the immediate vicinity of the wall by[13]

$$\alpha(z_M) = -\lambda \left(\frac{\partial T(z_M)}{\partial r}\right)_{r=0} = -\frac{a_1 \lambda}{-A^{1/3}} = -\frac{a_1 \lambda}{A^{1/3}} \frac{F_z^{1/2}}{\left[\int_0^{z_M} F_z^{1/2}\, dz_M\right]^{1/3}}\,. \tag{24}$$

The right hand side of Eq. (*24*) was obtained with the aid of Eqs (*14*) and (*19*). The parameter p, defined as the ratio of the local heat transfer coefficient α_m (corresponding to the case of identical beginning of the hydrodynamic and the thermal boundary layer, *i.e.* $z_M = 0$) to α_p determined by the instrument for the thermal flux

($i.e.$ at the point z_{Mn}) then equals

$$p = \frac{\alpha_{\mathrm{m}}}{\alpha_{\mathrm{p}}} = a_1 \, \Delta_{\mathrm{zp}}/a_{1\mathrm{p}} \, \Delta_{\mathrm{z}} = \left[a_1 \int_{z_{\mathrm{Mp}}}^{z_{\mathrm{M}}} F_{\mathrm{z}}^{1/2} \, \mathrm{d}z_{\mathrm{M}} / a_{1\mathrm{p}} \int_0^{z_{\mathrm{M}}} F_{\mathrm{z}}^{1/2} \, \mathrm{d}z \right]^{1/3} . \quad (25)$$

Respecting the fact that individual terms of the power series (*14*) are not functions of the coordinate z_{M}, the right hand side of Eq. (*25*) may be scaled by a_1, or $a_{1\mathrm{p}}$ to obtain finally for the parameter p the relation

$$p = \left[\int_{z_{\mathrm{Mp}}}^{z_{\mathrm{M}}} F_{\mathrm{z}}^{1/2} \, \mathrm{d}z_{\mathrm{M}} \Big/ \int_0^{z_{\mathrm{M}}} F_{\mathrm{z}}^{1/2} \, \mathrm{d}z_{\mathrm{M}} \right]^{1/3} . \quad (26)$$

The integrals on the right hand side of Eq. (*26*) may be solved numerically from the known course of the quantity F_{z} along the vessel's wall ($i.e.$ in the direction of coordinate z_{M}). This course may be expressed, using Eq. (*23*), from the knowledge of the velocity and the length scale $\bar{w}_{\mathrm{z,max}}$ or σ found by earlier described technique.

LIST OF SYMBOLS

A	constant in Eq. (*18*)
a	thermal conductivity, $\mathrm{m}^2 \, \mathrm{s}^{-1}$
a	exponent diffuzivity
a_{N}	N-th term in series (*14*)
b	width of radial baffle, m
b	exponent in Eq. (*8b*)
c_{f}	friction factor
D	vessel diameter, m
d	impeller diameter, m
$\mathbf{e}$	unit vector
F_{z}	derivative $(\partial \bar{w}_{\mathrm{z}}/\partial r)$ at the point $r = 0$, s^{-1}
H	liquid height at rest, m
H_2	height of lower edge of impeller blades over bottom, m
H'_2	height of disc of the turbine over bottom, m
h	height of impeller blade, m
j_{h}	factor of analogy between heat and momentum transfer
l_1	radial distance of thermocouple ***c*** from vessel wall, m
l_2	radial distance of thermocouple ***b*** and ***d***, m
N	summation index
n	frequency of revolution of impeller, s^{-1}
Nu	$= \alpha_a \sigma/\lambda$ Nusselt number
p	correction parameter

Pr	$= \nu/a$ Prandtl number
q	thermal flux, $W m^{-2}$
r	radial coordinate, m
Re	$= \bar{w}_{z,max}\,\sigma/\nu$ Reynolds number
Re_M	$= nd^2/\nu$ Reynolds number for mixing
St	$= Nu/(Re\,Pr)$ Stanton number
T	dimensionless temperature
t	temperature, K
t_0	wall temperature, K
t_∞	integral-mean temperature of liquid, K
$\bar{\mathbf{w}}$	local mean velocity, ms^{-1}
$\bar{\mathbf{w}}_k$	projection of mean velocity onto vertical plane, ms^{-1}
$\bar{w}_r$	radial component of mean velocity, ms^{-1}
$\bar{w}_z$	axial component of mean velocity, ms^{-1}
$\bar{w}_\varphi$	tangential component of mean velocity, ms^{-1}
$\bar{w}_{z,max}$	maximum value of $\bar{w}_z$ on radial profile in wall region (velocity scale), ms^{-1}
z	axial coordinate, m
z_M	axial coordinate with origin on horizontal plane of disc, m
α_m	experimental local heat transfer coefficient, $W m^{-2} K^{-1}$
α_a	heat transfer coefficient computed from analogy, $W m^{-2} K^{-1}$
α_p	local heat transfer coefficient determined by instrument for measuring heat flux, $W m^{-2} K^{-1}$
α	angle
β	angle
δ_z	thickness of hydrodynamic boundary layer, m
Δ_z	thickness of thermal boundary layer, m
β	angular coordinate
λ	thermal conductivity of liquid, $W m^{-1} K^{-1}$
ν	kinematic viscosity of liquid, $m^2 s^{-1}$
σ	radial coordinate of quantity $\bar{w}_{z,max}$ (length scale), m
$\bar{\tau}_0$	wall shear stress, Pa
ϱ	density of liquid, $kg m^{-3}$

REFERENCES

1. Askew W. S., Beckman R. B.: Ind. Eng. Chem., Process Des. Develop. *4*, 311 (1965).
2. Akse H., Beek W. J., Berkel van F. C., Graauw de J.: Chem. Eng. Sci. *22*, 135 (1967).
3. Le Lan A., Laguerie C., Angelino M.: Chem. Eng. Sci. *29*, 2021 (1974).
4. Le Lan A., Angelino M.: Chem. Eng. Sci. *29*, 1557 (1974).
5. Le Lan A., Angelino M.: Int. J. Heat Mass Transfer *18*, 163 (1975).
6. Stammers E.: *Thesis*. Technical University, Delft 1969.

7. Mizushina T., Ito R., Hiraoka S.: Paper presented at the V-th CHISA Congress, Prague, September 1975.
8. Baines W. D., Keffer J. F.: Int. J. Heat Mass Transfer *19*, 21 (1976).
9. Sitharanaya S., Subba R. K.: Can. J. Chem. Eng. *47*, 365 (1969).
10. Glauert M. B.: J. Fluid Mech. *1*, 625 (1956).
11. Rajaratnam N., Subramanya K.: J. Hyd. Res. *5*, 281 (1967).
12. Sigalla A.: Roy. Aero J. *62*, 873 (1958).
13. Knudsen J. G., Katz D. L.: *Fluid Dynamics and Heat Transfer.* McGraw Hill, New York 1958.
14. Fořt I., Vlček J., Cink M., Hrubý M.: This Journal *36*, 1546 (1971).
15. Fořt I., Podivínská J., Baloun R.: This Journal *34*, 959 (1969).
16. Micheev M. A.: *Osnovy Teploperedatchi.* Gos. Energ. Izd., Moscow, Leningrad 1949.
17. Strek F.: *Mieszanie i Meszalniki.* Wyd. Naukowotechniczne, Warsaw 1971.
18. Štěpánek V.: *Matematická statistika v chemii.* Published by SNTL, Prague 1964.

Translated by V. Staněk.